ACS APPLIED MATERIALS & INTERFACES

Research Article

www.acsami.org

Modification of Silicon Carbide Surfaces by Atmospheric Pressure Plasma for Composite Applications

Victor Rodriguez-Santiago,* Lionel Vargas-Gonzalez, Andres A. Bujanda, Jose A. Baeza, Michelle S. Fleischman, Jacqueline H. Yim, and Daphne D. Pappas

U.S. Army Research Laboratory, 4600 Deer Creek Loop, Aberdeen Proving Ground, Maryland 21005, United States

ABSTRACT: In this study, we explore the use of atmospheric pressure plasmas for enhancing the adhesion of SiC surfaces using a urethane adhesive, as an alternative to grit-blasting. Surface analysis showed that He–O_2 plasma treatments resulted in a hydrophilic surface mostly by producing SiO_x. Four-point bending tests and bonding pull tests were carried out on control, grit-blasted, and plasma-treated surfaces. Grit-blasted samples showed enhanced bonding but also a decrease in flexural strength. Plasma treated samples did not affect the flexural strength of the material and showed an increase in bonding strength. These results suggest that atmospheric pressure plasma treatment of ceramic materials is an effective alternative to grit-blasting for adhesion enhancement.

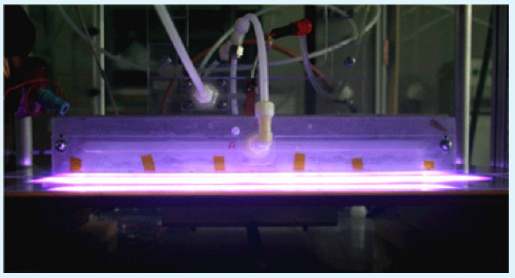

KEYWORDS: *silicon carbide, dielectric barrier discharges, bonding, surface modification, grit blasting*

1. INTRODUCTION

Ceramic materials are often used as high performance components in complex composite material structures. Ceramic composites and scaffolds are popular implant materials in the field of dentistry and orthopedics and are also used in structural applications (e.g., armor).[1,2] Silicon carbide is a highly studied ceramic because it possesses high strength-to-weight ratio and wear and corrosion resistance, as compared to other high performance ceramics. Adhesion improvement between metallic substrates (such as Mg or Al alloys)[3] and ceramic/polymer composites is often desired for structural applications as well.[2] However, bonding dissimilar materials, which can withstand high loads without delamination, remains a significant challenge.

Various surface treatment methods have been used to prepare ceramic materials for adhesion in composite structures. Among the techniques used, grit-blasting is the preferred method for enhancing bonding and improving their compatibility with dissimilar materials. This enhanced adhesion is generally achieved by increasing surface roughness. Although grit-blasting is effective at enhancing adhesion in ceramic materials, it can also cause damage to the surface which decreases the ultimate strength of the material. Other methods used to prepare ceramic surfaces include air abrasion at high pressure, ultrasonic cleaning,[4] laser treatments,[5] and CO_2 snow jets.[6] However, like grit-blasting, these methods can induce critical surface flaws into an already surface flaw-dominated material thus creating a need for other techniques that will not compromise the strength of the ceramic material.

Chemical methods, such as sol–gel silane treatments,[7] have also been used to provide chemical affinity between the ceramic surface and the adhesive. However, elaborate chemical treatments and waste generation are undesirable, from a production and manufacturing standpoint. While all these different approaches have been, in most cases, proven successful in removing surface residual impurities, the need for a process that is faster, less expensive, high throughput, and that will not negatively impact the strength of the ceramic material is needed.

Nonthermal atmospheric-pressure plasmas, specifically dielectric barrier discharges, have been extensively used for the surface treatment and modification of polymer materials due to the ease of formation of stable plasmas, low cost of operation, fast materials processing, and scalability.[8−11] However, the use of atmospheric pressure plasmas for the treatment of ceramic materials is scarce. Low pressure plasmas have been used on ceramic materials with the main foci on cleaning and etching[12,13] but also for enhancing adhesion.[14] Nonetheless, dielectric barrier discharges offer the opportunity to clean and modify the surface of ceramic materials with minimal waste and without reducing the strength of the material. In this study, helium/oxygen dielectric barrier discharges were used to treat SiC surfaces to investigate its effect on structural strength and adhesion as compared to grit-blasting. Surface analysis, bonding, and structural testing were carried out in order to elucidate the effects of each surface treatment. A urethane was used as a model adhesive to bond the plasma modified SiC samples in order to study their adhesion properties.

2. EXPERIMENTAL APPROACH

2.1. Surface Treatment and Materials. Plasma treatments were performed using a custom-built dielectric barrier discharge system.

Received: December 23, 2012
Accepted: May 2, 2013
Published: May 2, 2013

   dx.doi.org/10.1021/am303227q | ACS Appl. Mater. Interfaces 2013, 5, 4725−4730

The system consists of a flat aluminum ground electrode (area: 0.17 m^2) covered with a quartz plate, and a serrated stainless steel blade as the high voltage (HV) electrode, encased in a custom gas manifold and suspended over the ground electrode, as shown in Figure 1. The

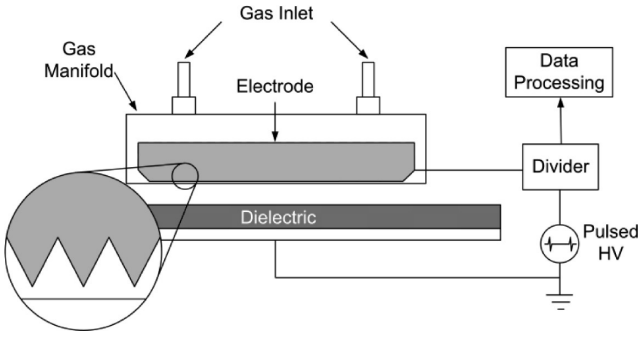

Figure 1. Schematic of dielectric barrier discharge system.

ground electrode is mounted in a motorized stage that allows it to move in the direction perpendicular to the HV electrode. The interelectrode distance can be adjusted over a wide range in order to fit samples of different thicknesses. In this study, the distance between the HV electrode and the surface of the samples was kept at 2 mm. The serrated blade HV electrode had the following dimensions: 31 cm in length and 0.6 mm thick. It had 7 teeth cm^{-1}, and the individual teeth were 0.6 mm long and 1 mm wide at the base. The system was equipped with a microsecond-pulsed power supply that generates pulses with a width of 30 μs at a duty cycle of 8%. The pulses had a peak voltage and power of 20 kV and 300 W, respectively. Voltage and current probes were used to monitor the corresponding waveforms. The flow rate of the carrier gas, in this case He (Praxair, 99.999%), was 200 cm^3 s^{-1} in order to obtain a stable discharge. Oxygen (Air Products, 99.999%) was used as reactive gas at a flow rate of 4 cm^3 s^{-1}.

Silicon carbide (SiC-N, BAE Systems-Vista, CA, USA) samples were cleaned in ultrasonic baths using acetone, methanol, and ethanol, respectively, for 10 min each and dried under nitrogen flow. For the grit-blasted samples, fused aluminum oxide grit was used with a nominal particle diameter of 180 μm (MSC Industrial Supply Co., USA). The grit gas pressure was 8.9×10^5 Pa (130 psi) through an aluminum nozzle of diameter 6.3 mm. The nozzle was held at a distance of 15 cm above the sample. Samples were blasted manually using a side to side sweeping motion once over a given area.

2.2. Surface Characterization. Wettability testing was carried out using a static water contact angle (WCA) setup using the sessile drop method, as described elsewhere.[15] Surface roughness of the samples was obtained using a Dimension 3100 microscope with a Nanoscope IV controller (Digital Instruments/Veeco) atomic force microscope (AFM). Root mean square (RMS) roughness values from 4 to 6 images, obtained from different locations on each sample, were averaged; outliers (high and low from each data set) were discarded in the reported average and standard deviations. Near surface compositional profiling was performed using the Kratos Axis Ultra X-ray photoelectron spectroscopy (XPS) system, equipped with a hemispherical analyzer. A 100 W monochromatic Al Kα (1486.7 eV) beam irradiated a 1 mm × 0.5 mm sampling area with a takeoff angle of 90°. Surface morphology was studied using a FEI NanoSEM in both field-emission and immersion modes at nominal accelerating voltages of 10–20 kV.

2.3. Structural and Bonding Testing. Flexural strength testing was conducted on the silicon carbide ceramic in accordance with ASTM standard C1161 4-point bending method. The testing was carried out using an Instron 1123 (Norwood, MA) electromechanical load frame. Thirty specimens of SiC, 5.1 cm^2 in area, were used as substrates. The SiC flexure bars were loaded into a fully articulating 4-point bend fixture with the 4 mm treated surface facing the tensile (bottom) direction, as shown in Figure 2. The specimens were loaded at a crosshead displacement rate of 0.5 mm min^{-1}, ensuring a flexural

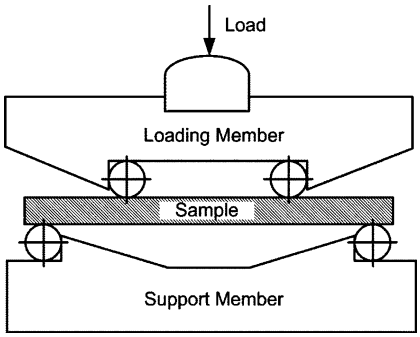

Figure 2. Schematic of a fully articulating four-point bend fixture for flexural strength testing.

strain rate of 1×10^{-4} s^{-1}. Thirty valid flexural tests were conducted for each condition (i.e., control, grit blasted, and plasma-treated).

Bonding adhesion performance was evaluated in a method similar to the ASTM standard F2258-05 (Standard Test Method for Strength Properties of Tissue Adhesives in Tension). After the subsequent plasma or grit blasting treatment, an Al grip tap with a 2.5 cm^2 base was bonded to each tile square using a commercially available one-step moisture cure polyurethane sealant (Sikaflex-252, Sika Corporation, Lyndhurst, NJ). A 0.5 mm diameter nylon fishing line was used to ensure a constant thickness bond line. The samples were placed under a weight and left to cure for one week in ambient conditions. The bonded test samples were evaluated using a load frame in tension (5500R, Instron, Norwood, MA), with the grip moving upward on the crosshead and the substrate locked in place on the base plate. The load frame was equipped with a 5 kN load cell. Ten samples from each condition were evaluated using a crosshead displacement of 0.5 mm s^{-1} to a maximum total displacement of 4 mm.

3. RESULTS AND DISCUSSION

3.1. Wettability and Surface Characterization. $He-O_2$ plasma treatment resulted in a decrease in water contact angles of SiC surfaces, as shown in Figure 3. Plasma treatments with

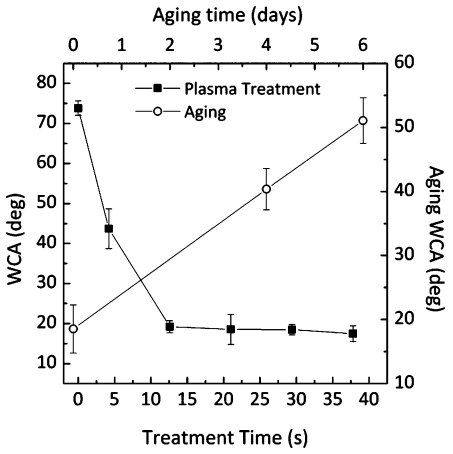

Figure 3. WCA as a function of plasma treatment time and aging, respectively. SiC samples were exposed to a $He-O_2$ discharge (2 vol % O_2).

He/O_2 plasma were performed under oxygen concentrations from 0 to 5%, with 2% providing the lowest contact angles. SiC surfaces exhibited more than 75% decrease in WCA after 12 s of plasma treatment, but no further decrease was observed with subsequent treatment. An aging study was performed to examine whether there were any post plasma changes of the surface properties. A rapid aging behavior was observed; a 2-

fold increase of the WCA occurred in six days after treatment. This aging behavior can be explained by the formation of a thin SiO_2-like layer on the surface of SiC after plasma treatment (XPS results). Immediately after plasma treatment, this SiO_2 layer is dehydroxylated, by the oxygen species in the plasma, which gives the plasma-treated samples a hydrophilic surface upon contact with water, according to a mechanism proposed by Habib et al. (and references therein).[16] After exposure to ambient humidity and adventitious contamination, the surface returns to a mostly Si−OH surface which gives it a more hydrophobic character, by acting as adsorption sites to organic contamination.[17] The grit-blasted sample had a contact angle of 50° after cleaning.

AFM images of control, grit-blasted, and plasma-treated SiC surfaces are shown in Figure 4. Control and plasma-treated

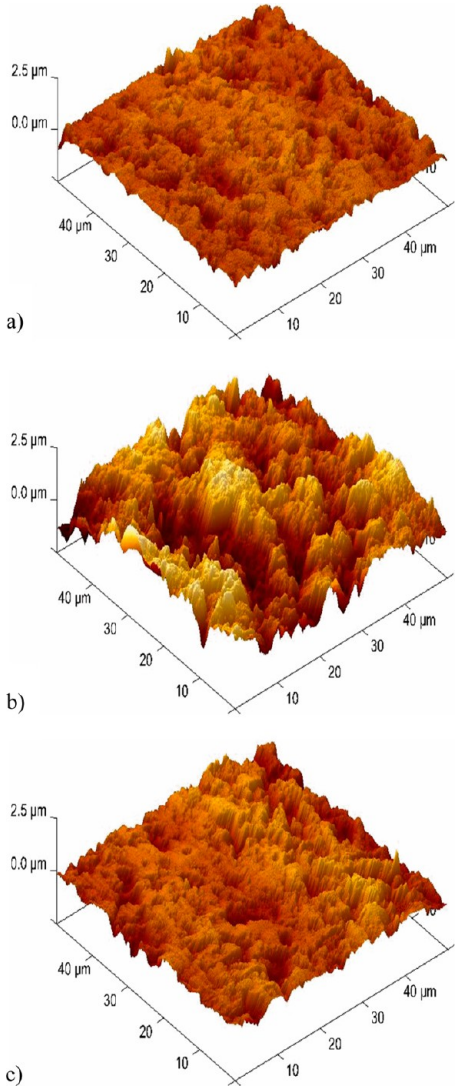

Figure 4. AFM images of (a) control, (b) grit-blasted (for 12 s), and (c) plasma-treated SiC surfaces.

samples (Figure 4a and c) show similar morphological features, showing only minor differences. The grit-blasted sample (Figure 4b) showed a significantly rougher surface with more distinct morphological features. RMS roughness values were obtained through AFM: 237.6 ± 40.8, 616.3 ± 61.1, and 286.8 ± 24.1 nm for control, grit-blasted, and plasma-treated samples, respectively. The roughness of the control and plasma-treated samples were statistically similar.

An examination of the chemical composition of the different samples was also performed via XPS, and results are presented in Table 1. All samples showed Si, C, and O as their main

Table 1. XPS Survey Results for Control, Grit-Blasted, and Plasma-Treated SiC Samples

sample	C (at %)	O (at %)	Si (at %)	Al (at %)	C/Si	Si:C:O
control	52.1	15.4	29.9	1.5	1.7	1:1.8:0.5
grit-blasted	33.4	28.0	23.7	14.9	1.4	1:1.3:1.1
plasma-treated	29.6	30.4	37.1	2.8	1.3	1:0.8:0.8

constituents, showing mainly the Si_{2p} peak at 100 eV, C_{1s} peak at 284.7 eV, and O_{1s} peak at 532 eV. Aluminum was also present in all samples; however, the grit-blasted sample had a relatively higher concentration. Although Al_2O_3 is used as a sintering agent in SiC ceramics (1−15 wt %),[18] the high concentration of Al suggests cross-contamination from the grit material (Al_2O_3). The control sample shows excess of carbon, most likely indicating that carbon contamination was not completely removed by the cleaning procedure. On the other hand, the grit-blasted sample shows a decrease in carbon content, closer to a stoichiometric ratio with Si, this as mechanical abrasion exposes the new surface. The increase in oxygen content compared to the control sample most likely comes from the grit material.

The plasma-treated sample shows a maximum Si content compared to either control or grit-blasted, and carbon content is decreased. It can be argued that the plasma treatment not only rids the surface of adventitious organic contamination but it also further oxidizes the surface. In order to corroborate this hypothesis, the high resolution scan for the Si_{2p} peak was investigated and presented in Figure 5. For all samples, the Si_{2p} peak could be deconvoluted into SiO_xC_y peaks as follows:[19] Si−C_4 at 99.9 eV, Si−O−C_3 at 100.7 eV, Si−O_2−C_2 at 101.4 eV, Si−O_3−C at 102.3 eV, and Si−O_4 at 103.4 eV. All peaks had fwhm of 1.2 or less. The control and grit-blasted samples showed very similar peaks, indicating that even before plasma treatment the surface contains a silicon oxycarbide layer. However, for the plasma-treated sample, the Si−O_4 peak at 103.4 eV was twice as intense as the control or grit-blasted, and the Si−C_4 peak appeared less intense. This clearly indicates that the He/O_2 plasma further oxidized the surface. Nonetheless, the fact that the Si−C_4 is present, even on the plasma-treated sample, indicates that this oxidized layer is very thin. The enhancement of this SiO_x layer on the plasma-treated surface will likely yield improved adhesion and bonding to the adhesive as silanol groups will readily react with isocyanate groups to form urethane linkages.

3.2. Flexural Testing. Flexural strength results for control, grit-blasted, and plasma-treated samples are presented in a Weibull plot, shown in Figure 6. Briefly, this plot represents the distribution of cumulative failure probabilities as a function of the applied tensile stress. The characteristic flexural strength, σ_0, for a given material is given by the strength at which the probability of failure is 63%. The slope of this plot is commonly known as the Weibull modulus, m, and it represents the spread of failure strengths; a high modulus indicates a narrow distribution of failure strengths.

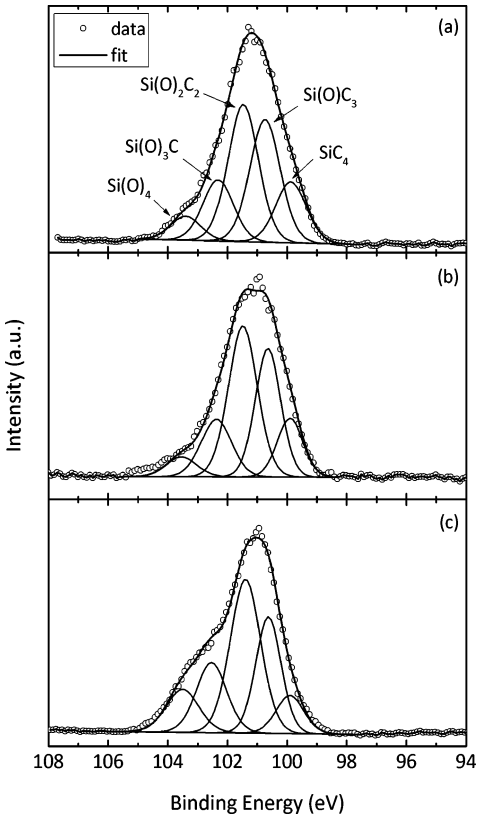

Figure 5. High resolution scan of the Si_{2p} peak of (a) control, (b) grit-blasted, and (c) plasma-treated SiC surfaces.

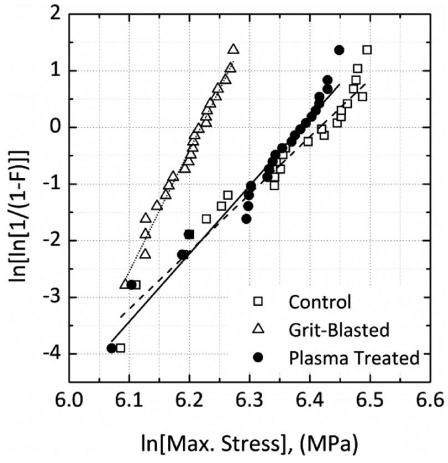

Figure 6. Weibull plot for the flexural strength tests on SiC.

A summary of flexural strength data obtained from Figure 6 is presented in Table 2. Flexural strength and Weibull modulus values for control samples were consistent with values reported in the literature.[20,21] Plasma-treated samples exhibited strength and modulus values similar to the control samples, indicating that plasma treatment does not negatively affect the strength of the material in a significant manner. That is, based on a sample population of 30 specimens, the characteristic strength values between control and plasma-treated samples are within the same 95% confidence interval (ASTM Standard C1239).

Table 2. Characteristic Flexural Strength and Weibull Modulus for Control, Grit-Blasted, and Plasma-Treated SiC Samples

sample	characteristic flexural strength, σ_0 (MPa)	Weibull modulus, m
control	608.7	10.2
grit-blasted	501.8	21.4
plasma-treated	591.6	12.0

On the other hand, grit-blasted samples showed a 17.6% decrease in maximum flexural strength compared to the control sample. This decrease is representative of the exacerbation of the preexisting flaws in the surface of the control samples or the creation of new flaws that become the dominant, strength-limiting flaw population. SEM fractography (not shown) of all specimen sets (control, grit-blasted, and plasma-treated) showed that the origins of fracture were surface flaws. The abrasive nature of grit blasting gives rise to tensile stress fields where the maximum stress is below the surface of the material. The stresses are relieved through the introduction of new surface defects or through growth in existing defects, both of which cause a decrease in the strength of the material. Similar effects have been observed in ultrasonically machined ceramics.[22]

The increase in Weibull modulus for the grit-blasted sample, compared to control and plasma-treated samples, is possibly due to an increase in the homogeneity of surface flaw shapes and has been observed in other ceramic systems subjected to ablative laser treatments.[23] The results from flexural testing show a benefit in flaw population consistency caused by plasma exposure without a corresponding drop in characteristic strength. The greater change in variability expressed in the grit-blasted specimens also shows a significant reduction in strength, further limiting their use in high stress environments.

3.3. Bonding Testing. Ten samples for each treatment condition were tested, and a single curve for each condition was generated through averaging the results of the distinct tests. These results were plotted and are presented in Figure 7. The calculated average and deviation values are listed in Table 3.

The control samples exhibited a high initial elastic response, reaching a maximum tensile strength near 0.20 mm of extension, dropping slightly to reach a plateau where another 0.25−0.30 mm of extension occurred before unloading. The point of unloading coincides with the initialization of bond

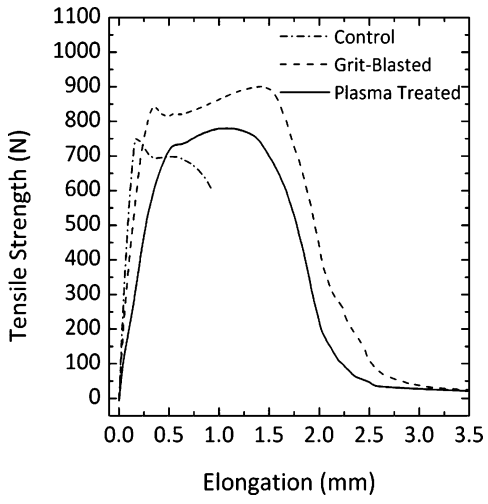

Figure 7. Adhesive bonding strength as a function of treatment condition.

dx.doi.org/10.1021/am303227q | ACS Appl. Mater. Interfaces 2013, 5, 4725−4730

Table 3. Measured Bond Strengths and Elongation for Each Surface Treatment Condition

sample	maximum bonding strength (N)	maximum elongation before failure (mm)
control	752.9 ± 77.8	0.5
grit-blasted	937.3 ± 56.8[a]	1.3
plasma-treated	780.2 ± 45.6[a]	1.12

[a]Failure did not occurr at the surface/adhesive interface.

failure. For most of the control samples, the adhesive bond failure occurred at the ceramic/adhesive interface, as shown in Figure 8a.

The grit-blasted samples exhibited a similar initial response to the control sample; however, it was displaced to a higher elongation (0.30 mm extension). In addition, the bond line was found to be tougher, with the samples being able to achieve nearly 1.50 mm of extension before initialization of bonding failure. Many of the test coupons from the grit-blasted samples failed at the metal grip tab, implying that the higher roughness values had a positive effect on the strength of the ceramic/adhesive interface (Figure 8b). As a result of this improved interface, an increase in the plastic deformation was seen in the strength and toughness.

The plasma-treated samples extended further to ~0.60 mm before the initiation of yielding. Overall, extension occurs through 1.5 mm of extension before initialization of bonding failure, similar to the grit-blasted sample. As shown in Figure 8c, nearly all samples exhibited adhesive failure at the metal grip tab. Since both the grit-blasted and plasma-treated samples experienced failure at the tab/adhesive interface, the maximum tensile strength is not indicative of the strength of the ceramic/adhesive interface. However, the extent of elongation prior to failure provides some clues about bonding. The increased elongation of the grit-blasted sample follows the increased roughness which provides both mechanical interlocking and a larger surface area to interact with the adhesive. This seems reasonable since chemically (Figure 5) the control and grit-blasted samples are similar.

On the other hand, the increased elongation and enhanced toughness exhibited by the plasma-treated SiC could be due to covalent bonds formed from oxidized functional groups (mainly silanols) reacting with the adhesive. These reactions, between silanol groups and the isocyanate adhesive could lead to the formation of an interface comprised of an elastomeric cross-linked networked of polyurethanes. Another explanation for the increased adhesion, based on works of Wehlack et al. and Johlitz et al.,[24−26] could be the result of incomplete curing of the adhesive, yielding a less cross-linked system and higher concentration of free oligomers. This incomplete cure process can be caused from a variety of factors such as preferential adsorption or immobilization of the adhesive species due to the introduction of new reactive groups on the substrate surface. These new groups can affect the cure kinetics of the adhesive by altering the stoichiometry of reactive groups, specifically isocyanates and hydroxyls (NCO:OH). This can bring about changes in crystallization, phase separation, and molecular arrangements, ultimately influencing the mechanical response of the adhesive.

Finally, although increased adhesion is obtained by the grit blasting process, it comes at the expense of reduced strength caused by the introduction and exacerbation of surface flaws.

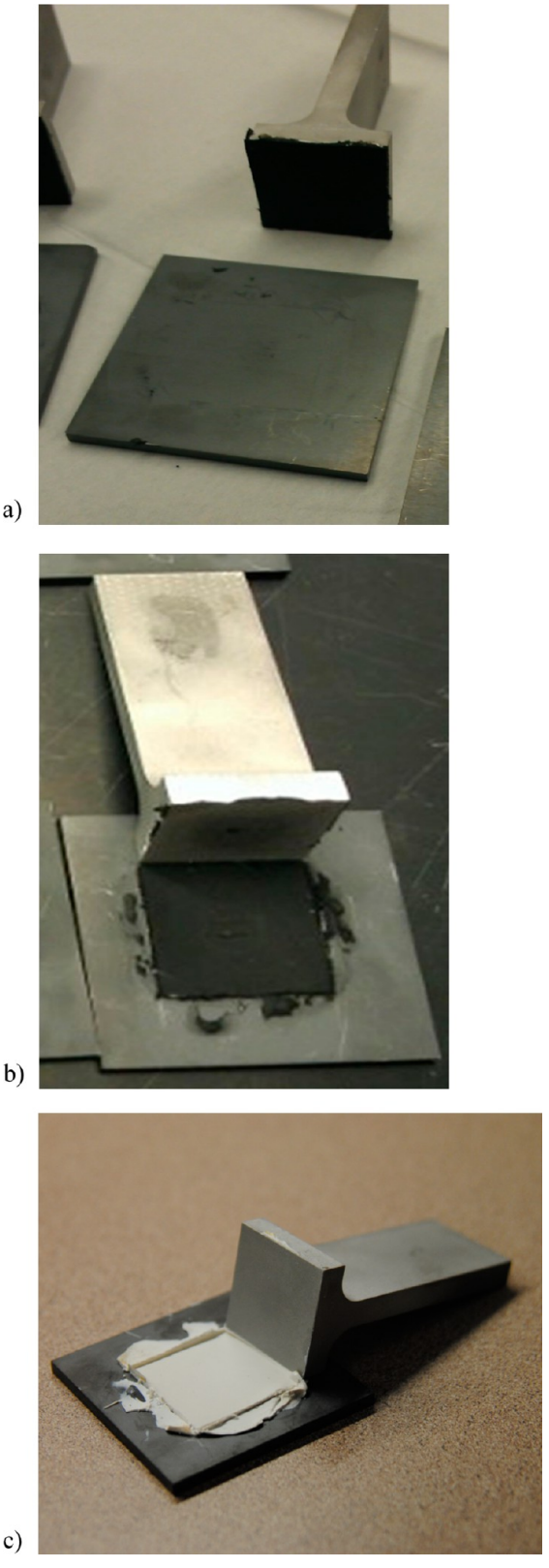

Figure 8. Test coupons after adhesion bond testing for (a) control, (b) grit-blasted, and (c) plasma-treated samples.

Plasma treatment, on the other hand, can potentially provide similar adhesion without negative effects to the strength of the material. This makes atmospheric pressure plasma processing an attractive alternative for bonding hybrid composites.

4. CONCLUSIONS

Silicon carbide surfaces were treated by atmospheric pressure plasma and grit blasting and their chemical, morphological, and structural properties compared to as-received specimens. Plasma treatment did not promote significant morphology changes; however, it changed the chemical composition of the surface as evidenced by contact angle and XPS measurements. Grit blasting increased the surface roughness almost 3-fold. Flexural strength testing revealed that plasma treatments do not affect the ultimate strength of the materials detrimentally. In contrast, grit-blasted samples experienced approximately 17% decrease in flexural strength caused by the exacerbation of existing surface flaws during grit-blasting. Bonding tests revealed strengths between the grit blasted and plasma-treated samples are similar. However, since the failures occur at the interface between the metal tab and the adhesive, the strengths measured are indicative of the performance of the metal/adhesive interface, and thus should be similar in value. While the testing shows that the bond between the ceramic and adhesive has improved with respect to the as-received specimens, another mechanical test method will be pursued in the future to interrogate the ceramic/adhesive boundary. While these results are not fully conclusive, the results suggest that atmospheric pressure plasmas are a cost-effective, non-destructive alternative surface treatment for ceramic materials for composite bonding applications.

AUTHOR INFORMATION

Corresponding Author

*Telephone: 1-410-306-3307. Fax: 1-410-306-0829. E-mail: victor.rodriguez31@us.army.mil.

Notes

The authors declare no competing financial interest.

ACKNOWLEDGMENTS

This research was supported in part by an appointment to the Postgraduate Research Participation Program at the U.S. Army Research Laboratory administered by the Oak Ridge Institute for Science and Education through an interagency agreement between the U.S. Department of Energy and USARL.

REFERENCES

(1) Habraken, W. J. E. M.; Wolke, J. G. C.; Jansen, J. *Adv. Drug Delivery Rev.* **2007**, *59*, 234−248.
(2) Zaera, R. In *Impact Engineering of Composite Structures*; Abrate, S., Ed.; Springer: Vienna, 2011; pp 305−403.
(3) Vargas-Gonzalez, L. R.; Walsh, S. M.; Pappas, D. D. *Polym. Compos.* **2012**, *33*, 207−214.
(4) Attia, A.; Kern, M. *J. Adhes. Dent.* **2011**, *13*, 561−567.
(5) Lawrence, J.; Li, L.; Spencer, J. T. *Appl. Surf. Sci.* **1999**, *138−139*, 388−393.
(6) Sherman, R.; Hirt, D.; Vane, R. *J. Vac. Sci. Technol., A* **1994**, *12*, 1876.
(7) Tanoglu, M.; Mcknight, S. H.; Palmese, G. R.; Gillespie, J. W. *Int. J. Adhes. Adhes.* **1998**, *18*, 431−434.
(8) Tendero, C.; Tixier, C.; Tristant, P.; Desmaison, J.; Leprince, P. *Spectrochim. Acta, Part B* **2006**, *61*, 2−30.
(9) Bogaerts, A.; Neyts, E.; Gijbels, R.; van der Mullen, J. *Spectrochim. Acta, Part B* **2002**, *57*, 609−658.
(10) Shenton, M. J.; Stevens, G. C. *J. Phys. D: Appl. Phys.* **2001**, *34*, 2761−2768.
(11) Rodriguez-Santiago, V.; Bujanda, A. a.; Stein, B. E.; Pappas, D. D. *Plasma Processes Polym.* **2011**, *8*, 631−639.
(12) Yi, C. H.; Jeong, C. H.; Lee, Y. H.; Ko, Y. W.; Yeom, G. Y. *Surf. Coat. Technol.* **2004**, *177−178*, 711−715.
(13) Vesel, A.; Mozetic, M.; Drenik, A.; Milosevic, S.; Krstulovic, N.; Balat-Pichelin, M.; Poberaj, I.; Babic, D. *Plasma Chem. Plasma Process.* **2006**, *26*, 577−584.
(14) Neyman, E.; Dillard, J. D.; Dillard, D. A. *J. Adhes.* **2006**, *82*, 331−353.
(15) Pappas, D. D.; Bujanda, A. a.; Orlicki, J. a.; Jensen, R. E. *Surf. Coat. Technol.* **2008**, *203*, 830−834.
(16) Habib, S. B.; Gonzalez, E.; Hicks, R. F. *J. Vac. Sci. Technol., A* **2010**, *28*, 476−485.
(17) Williams, T. S.; Hicks, R. F. *J. Vac. Sci. Technol., A* **2011**, *29*, 041403−1−7.
(18) Mulla, M. A.; Krstic, V. D. *Acta Metall. Mater.* **1994**, *42*, 303−308.
(19) Soraru, G. D.; D'Andrea, G.; Glisenti. *Mater. Lett.* **1996**, *27*, 1−5.
(20) Vargas-Gonzalez, L.; Speyer, R. F.; Campbell, J. *Int. J. Appl. Ceram. Technol.* **2010**, *7*, 643−651.
(21) Rixecker, G.; Wiedmann, I.; Rosinus, A.; Aldinger, F. *J. Eur. Ceram. Soc.* **2001**, *21*, 1013−1019.
(22) Jianxin, D.; Taichiu, L. *J. Eur. Ceram. Soc.* **2002**, *22*, 1235−1241.
(23) Meeker, J.; Segall, A. E.; Semak, V. V. *J. Laser Appl.* **2010**, *22*, 7−12.
(24) Wehlack, C.; Possart, W. Formation, structure and morphology of polyurethane−metal interphases. In *5th International EEIGM/AMASE/FORGEMAT Conference on Advanced Materials Research:*, Nancy, France, Nov 4−5, 2009; p 012003.
(25) Wehlack, C.; Possart, W.; Kruger, J. K.; Muller, U. *Soft Mater.* **2007**, *5*, 87−134.
(26) Johlitz, M.; Diebels, S.; Possart, W. *Arch. Appl. Mech.* **2012**, *82*, 1089−1102.